Research Paper https://doi.org/10.7733/jnfcwt.2022.041

Evaluation of Americium Solubility in Synthesized Groundwater: Geochemical Modeling and Experimental Study at Over-Saturation Conditions

Hee-Kyung Kim* and Hye-Ryun Cho
Korea Atomic Energy Research Institute, 111, Daedeok-daero 989beon-gil, Yuseong-gu, Daejeon 34057, Republic of Korea

(Received October 24, 2022 / Revised October 31, 2022 / Approved November 4, 2022)

The solubility and species distribution of radionuclides in groundwater are essential data for the safety assessment of deep underground spent nuclear fuel (SNF) disposal systems. Americium is a major radionuclide responsible for the long-term radiotoxicity of SNF. In this study, the solubility of americium compounds was evaluated in synthetic groundwater (Syn-DB3), simulating groundwater from the DB3 site of the KAERI Underground Research Tunnel. Geochemical modeling was performed using the ThermoChimie_11a thermochemical database. Concentration of dissolved Am(III) in Syn-DB3 in the pH range of 6.4–10.5 was experimentally measured under over-saturation conditions by liquid scintillation counting over 70 d. The absorption spectra recorded for the same period suggest that Am(III) colloidal particles formed initially followed by rapid precipitation within 2 d. In the pH range of 7.5–10.5, the concentration of dissolved Am(III) converged to approximately 2×10^{-7} M over 70 d, which is comparable to that of the amorphous $AmCO_3OH$(am) according to the modeling results. As the samples were aged for 70 d, a slow equilibrium process occurred between the solid and solution phases. There was no indication of transformation of the amorphous phase into the crystalline phase during the observation period.

Keywords: Americium, Groundwater, Radionuclide migration, Solubility, Colloidal particle, Thermochemical data

*Corresponding Author.
Hee-Kyung Kim, Korea Atomic Energy Research Institute, E-mail: hkim11@kaeri.re.kr, Tel: +82-42-866-6294

ORCID
Hee-Kyung Kim http://orcid.org/0000-0001-5840-7194 Hye-Ryun Cho http://orcid.org/0000-0002-1293-6653

This is an Open-Access article distributed under the terms of the Creative Commons Attribution Non-Commercial License (http://creativecommons.org/licenses/by-nc/3.0) which permits unrestricted non-commercial use, distribution, and reproduction in any medium, provided the original work is properly cited

1. Introduction

The study of the chemical behavior of radionuclides under geochemical conditions is essential for long-term safety assessment of the deep geological disposal of spent nuclear fuel (SNF) [1]. The most probable migration path of radionuclides is through groundwater flow [2]. Radionuclides interact with various organic and inorganic components in groundwater as well as with mineral surfaces and colloidal particles [3-5]. The concentration of dissolved radionuclides in groundwater is the critical initial data that determines the maximum quantity to be considered for radionuclide interactions with environmental materials, including surrounding rocks. For a reliable evaluation of radionuclide migration through the geosphere to the biosphere, different local geochemical conditions as well as temporal variations due to the long-term evolution of the disposal system should be considered. These diverse spatial and temporal variations make it difficult to experimentally determine radionuclide solubilities and interactions with environmental materials.

International efforts have been devoted to establishing a reliable thermochemical database (TDB) for geochemical modeling of radionuclide behavior under diverse conditions. The selected data in the NEA-TDB [6] are renowned as reliable international standard data, but the data listed in the NEA-TDB are limited. The ThermoChimie TDB by Andra accepted thermodynamic data from the NEA-TDB and amended more data, even with low reliability, to better describe the systems of interest [7-8]. The ThermoChimie TDB was used for safety assessment of the Olkiluoto repository in Finland [9]. The ThermoChimie_11a version was updated in 2021, accommodating the NEA-TDB 2020 update. The reliability of the geochemical modeling results depends on the reliability of the thermodynamic data used and the comprehensiveness of the database. In addition, geochemical modeling results should be evaluated in conjunction with the experimental results.

Americium is one of the major radionuclides responsible for the long-term radiotoxicity of SNF. The ^{241}Am (half-life = 432.7 years) isotope is a relevant element in the radiotoxicity of SNF, as it is continuously generated and accumulated in SNF by the β-decay of ^{241}Pu [10-11]. ^{241}Am emits alpha (5.49, 5.44 MeV) and gamma rays (59.5 keV), and is converted to ^{237}Np (α-emitting nuclide) [12]. It is a highly radioactive element with a specific activity of 126.9 GBq·g^{-1} and can be easily quantified in the sub-nanomolar range using radio-analytical methods. Americium is stable in the +3 oxidation state under a wide range of aqueous solution conditions [2]. Thermochemical data for Am(III), a representative of +3 actinides and lanthanides, are relatively well described in the NEA-TDB and ThermoChimie. Recently, we reported detailed information on the spectroscopic properties of Am(III) species [13-15]. UV-Vis absorption and time-resolved laser-induced fluorescence spectroscopy are useful for Am(III) speciation.

In this study, dissolved americium concentrations and species distributions were examined under synthetic groundwater conditions (Syn-DB3), simulating groundwater from the DB3 site in the KAERI Underground Research Tunnel (KURT). Geochemical modeling was performed using the TheroChimie_11a TDB. Absorption and luminescence spectroscopy were used to monitor the evolution of species and colloidal particles in the samples. The solubility of americium in Syn-DB3 groundwater was measured using liquid scintillation counting (LSC) under oversaturated conditions. The experimentally measured values were compared with those predicted using geochemical modeling. Probable americium solid phases formed in the Syn-DB3 groundwater are discussed.

2. Methods

2.1 Geochemical Modeling

The solubility curves of americium were calculated using the Act2 module of the commercial GWB program

Table 1. Chemical composition of Syn-DB3 groundwater

Components	Syn-DB3 ($mol \cdot L^{-1}$)
pH	9.03
Na^+	1.66×10^{-3}
Ca^+	1.32×10^{-4}
K^+	1.23×10^{-5}
Mg^{2+}	1.07×10^{-5}
SiO_2	1.28×10^{-4}
HCO_3^-	1.38×10^{-3}
Cl^-	4.96×10^{-5}
SO_4^{2-}	5.74×10^{-5}
F^-	4.04×10^{-4}

(2022 Standard). A pH range of 6–11 was set to include the general groundwater pH range. As summarized in Table 1, the major ions contained in the Syn-DB3 groundwater were considered for modeling. The background ionic strength of the Syn-DB3 groundwater was calculated as 1.5 $mmol \cdot kg^{-1}$, which has an insignificant effect on the activity of ions; therefore, the molarity itself was used as the activity. In the case of silicate, carbonate, and sulfate ions, 'speciate over x-y' was set to consider the degree of dehydrogenation according to pH change. The temperature and pressure were set at 25℃ and 1.0 bar, respectively. The aqueous species distribution of Am in the Syn-DB3 groundwater was simulated using the GWB React module. When the pH was varied from 6 to 11, the redox potential (Eh) value was fixed at 0.2 V.

2.2 Sample Preparation

Syn-DB3 was prepared to simulate the domestic groundwater sampled at the DB3 site in KURT (Table 1). Only the major components of the KURT DB3 groundwater were considered. Chemicals used for the preparation were NaF (99.99%), $Ca(OH)_2$ (99.995%), KCl (> 99.0%), $Mg(OH)_2$ (> 99.0%), $Na_2SiO_3 \cdot 5H_2O$ (> 95%), NaCl (99.5%), $CaSO_4$ (99%), HF (99.99%) from Sigma-Aldrich. Syn-DB3 was prepared in air, indicating that the conditions were oxidative and the pH was 9.03.

^{241}Am (Amersham, 1986, YD8886, AMS 1LY) was purified using a cation exchange resin (AG 50W×8, Bio-rad, 200–400 mesh, 1.7 $meq \cdot ml^{-1}$ resin bed), as described previously [13-14]. The ^{241}Am stock solution was prepared in 0.1 M $HClO_4$ solution, and the concentration was determined to be 5.7 mM by LSC and gamma- and alpha-spectrometry [13].

Americium samples in Syn-DB3 groundwater were prepared by diluting the Am(III) stock solution with Syn-DB3 in two steps. In the first step, 5.7 mM Am(III) stock solution in 0.1 M $HClO_4$ was diluted to 100 μM Am(III) in Syn-DB3. In the second step, 10 mL of 11.8 μM Am (III) in Syn-DB3 was prepared from the diluted solution. After the second dilution, the pH of Am(III) in the Syn-DB3 solution was 7.5. To vary the pH condition of the samples, the second dilutions were performed with addition of small volume (0.5–4.5 μL) of 0.2 M $HClO_4$ (ULTREX II, Ultrapure reagent, JT Baker) or 0.1 M NaOH (Semiconductor grade, 99.99% trace metals basis, Sigma-Aldrich). The pH of the samples was measured using a glass combination electrode (Orion™, Ross Ultra) when preparing them. Am(III) samples in Syn-DB3 were prepared under five different pH conditions: 6.4, 7.5, 8.4, 8.7, and 10.5. Am(III) solution (11.8 μM) in 0.1 M $HClO_4$ (pH 1) was also prepared from the first diluted solution as a reference sample. Two milliliters of each sample were transferred into a quartz cell with a screw cap for absorption measurements, and the remaining 8 mL of the sample was transferred into a centrifuge tube (Oak Ridge high-speed PPCO centrifuge tube, 10 mL, Nalgene) for quantification of Am(III) in supernatant after centrifugation. All the sample preparation procedures were performed in an argon-filled glove box to avoid CO_2 dissolution.

Precaution! ^{241}Am is highly radioactive (specific activity = 126.9 $GBq \cdot g^{-1}$). This should be handled carefully under proper protection in radiation-controlled areas. The

concentrated ^{241}Am solution was handled in a fume hood or glovebox equipped with high-efficiency particulate air filters. During the sample purification and preparation process, the probable surrounding contamination was frequently checked using a gamma meter and a surface contamination detection method. The stability of the storage container of the ^{241}Am stock solution was an issue for long-term storage, as the erosion of plastic containers was observed over several years. This is likely due to the radicals generated by the alpha particles emitted from ^{241}Am. In particular, Teflon is weak against alpha particles, making it unsuitable for long-term storage. Currently, a quartz cell with a screw cap made of polyether ether ketone is used as a storage container for purified stock ^{241}Am.

2.3 UV-Vis Spectrophotometry

The absorption spectra of Am(III) were acquired using a spectrophotometer (Cary 5000, Agilent) equipped with a temperature controller. Quartz cells with beam path lengths of 1 cm were used. The absorption was scanned in the range of 525–495 nm with a spectral resolution of 0.1 nm, a spectral bandwidth of 0.5 nm, and an acquisition time of 1 s. Samples in the quartz cell were stored at room temperature (20–30℃ due to seasonal climate change) for aging-dependent measurements over 69 d, and the absorption measurements were conducted at 25℃ (deviation < ± 0.2℃).

2.4 TRLFS

The luminescence spectra of Am(III) samples were acquired using a TRLFS system [14, 16]. An Nd-YAG pumped OPO system (Vibrant B, OPOTEK Inc.) was employed as a wavelength-tunable nanosecond pulsed laser source. The excitation wavelength was chosen between 503.0 and 506.3 nm (2.3 mJ) as per the maximum absorption wavelength (λ_{max}) of each sample. Emissions were detected using an intensified CCD (ICCD) (iStar, Andor Technology) after a spectrograph (SR-303i, Andor Technology). All measurements were performed at 25℃ and controlled using a thermostat (Q-pod, Quantum Northwest).

2.5 Quantification of Am(III) in Supernatants

A liquid scintillation counter (LSC, TriCarb4910TR, PerkinElmer) was used to measure the Am(III) concentration in the solution. To quantify the Am(III) concentration in the supernatant of Am(III)_Syn-DB3 samples, the samples in centrifuge tubes were centrifuged at 18,000 rpm for 1 h. Ten microliters of each sample was taken from the upper part of the supernatant and mixed with 300 μL of 0.1 M HNO_3 in 20 mL polyethylene LSC vials to acidify Am(III), because LSC measurements for the solutions at high pH tend to be erroneous. The acidified Am(III) samples were mixed with 15 mL of LSC cocktail (Ultima Gold AB, PerkinElmer). The LSC was measured for 10 min using an alpha and beta discriminator.

The concentration of Am(III) was calculated using Equation (1) from the radioactivity (counts/s = Bq) obtained from LSC measurements.

$$A(Bq) = mole \cdot N_A \cdot \ln 2 / T_{1/2} \quad (1)$$

where A is the measured radioactivity value, N_A is the Avogadro number (6.02×10^{23}/mole), and $T_{1/2}$ is the half-life (s) of ^{241}Am. The first daughter of ^{241}Am is ^{237}Np (half-life = 2.14×10^{6} y), which undergoes alpha decay, but its half-life is 10^4 times longer than that of ^{241}Am, so the radioactivity value emitted from the daughter was not taken into account.

3. Results and Discussion

3.1 Geochemical Modeling Results

Geochemical modeling was conducted to estimate the solubility curves and dissolved species distributions of americium under the Syn-DB3 condition in the pH range

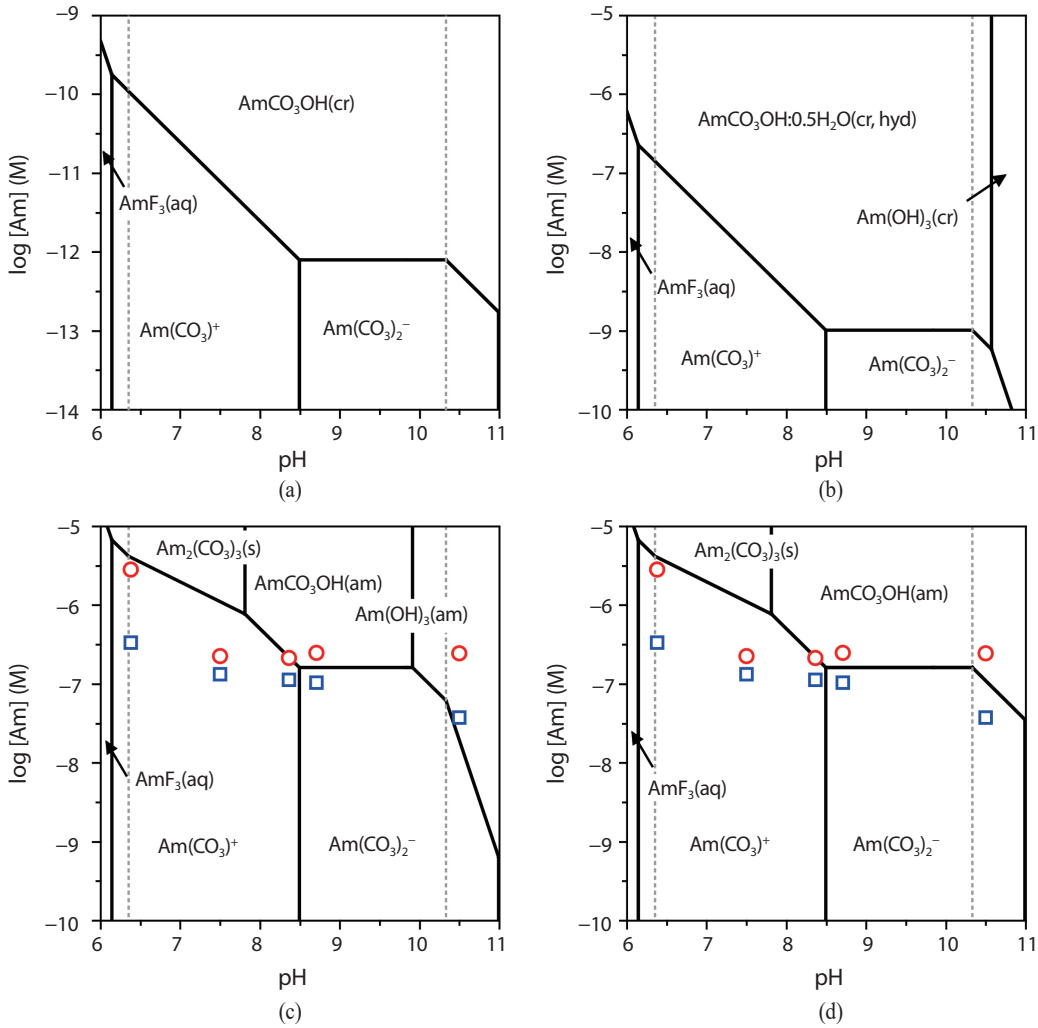


Fig. 1. Geochemical modeling results of americium solubility in Syn-DB3 groundwater condition. ThermoChimie_11a TDB from Andra was used as input DB for the modeling in (a). Solubility curves evaluated excluding the formation of (b) crystalline $AmCO_3OH$(cr); (c) crystalline $AmCO_3OH$(cr), $AmCO_3OH:0.5H_2O$(cr, hyd), and $Am(OH)_3$(cr); and (d) crystalline $AmCO_3OH$(cr), $AmCO_3OH:0.5H_2O$(cr, hyd), $Am(OH)_3$(cr), and $Am(OH)_3$(am). In (c) and (d), experimentally determined americium concentrations in the supernatants of Am_Syn-DB3 are denoted with blue rectangles and red circles, which were measured after 5 and 70 d of sample preparations, respectively. The vertical dashed lines represent the dehydrogenation reactions of the carbonate ion ($H_2CO_3 \leftrightarrows HCO_3^- + H^+ \leftrightarrows CO_3^{2-} + 2H^+$).

of 6–11 (Figs. 1 and 2). ThermoChimie_11a TDB from Andra was used as the input DB. In Tables 2 and 3, the thermodynamic data of the aqueous and solid americium species relevant to the Syn-DB3 groundwater conditions as in Figs. 1 and 2 are listed. Except for AmF_3, $AmSiO(OH)_3^{2+}$ and $AmCO_3OH$(cr), all other thermodynamic data were adapted from OECD NEA Chemical Thermodynamic Data Vol. 5 [2] and Vol. 14 [6]. The crystalline phases of $AmCO_3OH:0.5H_2O$(s), $AmCO_3OH$(s), and $Am_2(CO_3)_3$(s) were not defined in ThermoChimie_11a, whereas they were defined as hydrated crystalline $AmCO_3OH:0.5H_2O$ (cr, hyd), amorphous $AmCO_3OH$(am), and amorphous $Am_2(CO_3)_3$(am) in the NEA-TDB. In this study, we used the NEA-TDB notation. In the NEA-TDB project, Am(III) was exclusively reviewed as a representative actinide in the +3 oxidation state. They categorized Am(III), Cm(III),

Table 2. Thermodynamic data of aqueous Am(III) complexes relevant in KURT DB3 groundwater listed in ThermoChimie_11a

Ligand	Species	Reaction	logK^{o}
OH^-	$Am(OH)^{2+}$	$Am^{3+} + H_2O \leftrightarrows Am(OH)^{2+} + H^+$	−7.20 ± 0.50*
	$Am(OH)_2^+$	$Am^{3+} + 2H_2O \leftrightarrows Am(OH)_2^+ + 2H^+$	−15.10 ± 0.70*
	$Am(OH)_3$	$Am^{3+} + 3H_2O \leftrightarrows Am(OH)_3 + 3H^+$	−26.20 ± 0.50*
CO_3^{2-}	$Am(CO_3)^+$	$Am^{3+} + CO_3^{2-} \leftrightarrows Am(CO_3)^+$	7.90 ± 0.40**
	$Am(CO_3)_2^-$	$Am^{3+} + 2CO_3^{2-} \leftrightarrows Am(CO_3)_2^-$	12.60 ± 0.60**
	$Am(CO_3)_3^{3-}$	$Am^{3+} + 3CO_3^{2-} \leftrightarrows Am(CO_3)_3^{3-}$	14.60 ± 1.00**
	$Am(HCO_3)^{2+}$	$H^+ + Am^{3+} + CO_3^{2-} \leftrightarrows Am(HCO_3)^{2+}$	13.43 ± 0.55*
F^-	AmF^{2+}	$Am^{3+} + F^- \leftrightarrows AmF^{2+}$	3.40 ± 0.40*
	AmF_2^+	$Am^{3+} + 2F^- \leftrightarrows AmF_2^+$	5.80 ± 0.20*
	AmF_3	$Am^{3+} + 3F^- \leftrightarrows AmF_3$	10.82
$Si(OH)_4$	$AmSiO(OH)_3^{2+}$	$Am^{3+} + Si(OH)_4 \leftrightarrows AmSiO(OH)_3^{2+} + H^+$	−2.31 ± 0.13
SO_4^{2-}	$Am(SO_4)^+$	$Am^{3+} + SO_4^{2-} \leftrightarrows Am(SO_4)^+$	3.50 ± 0.30*

*Adapted from NEA-TDB

**Recalculated from NEA-TDB

Table 3. Thermodynamic data of solid americium species relevant to KURT DB3 groundwater condition listed in ThermoChimie_11a

Dissolution of Am(III) solid	log $K_{s,0}^{o}$
$AmCO_3OH(cr) + H^+ \leftrightarrows Am^{3+} + CO_3^{2-} + H_2O$	−11.51 ± 1.14
$AmCO_3OH{:}0.5H_2O(cr, hyd)^{**} + H^+ \leftrightarrows Am^{3+} + CO_3^{2-} + 1.5H_2O$	−8.4 ± 0.50*
$AmCO_3OH(am)^{**} + H^+ \leftrightarrows Am^{3+} + CO_3^{2-} + H_2O$	−6.2 ± 1.00*
$Am_2(CO_3)_3(am)^{**} \leftrightarrows 2Am^{3+} + 3CO_3^{2-}$	−33.4 ± 2.20*
$Am(OH)_3(cr) + 3H^+ \leftrightarrows Am^{3+} + 3H_2O$	15.6 ± 0.60*
$Am(OH)_3(am) + 3H^+ \leftrightarrows Am^{3+} + 3H_2O$	16.9 ± 0.80*

*Adapted from NEA-TDB

**Phases as defined in the NEA-TDB

Nd(III), and Eu(III) in an analogue element in evaluating the chemical thermodynamic data, because their chemical behaviors are similar due to their close ionic radii (Am^{3+}:1.10 Å, Cm^{3+}:1.09 Å, Nd^{3+}:1.11 Å, Eu^{3+}:1.07 Å) [13]. However, the redox behavior and solubility of isostructural solid compounds can be considerably different for each element; thus, they must be evaluated separately [2].

Experimentally determined solubilities tend to deviate considerably from each other and are highly dependent on the experimental conditions as well as the crystallinity of the solid compounds [2]. The dissolution of solid compounds at under-saturation conditions accompanies hydration of the surface in contact with the solution, by which the crystalline property is altered and finally becomes amorphous at the interface with the solution prior to dissolution. Thus, modeling results based solely on thermodynamic data may not accurately reflect reality. To consider crystallinity-dependent solubility, modeling was conducted stepwise,

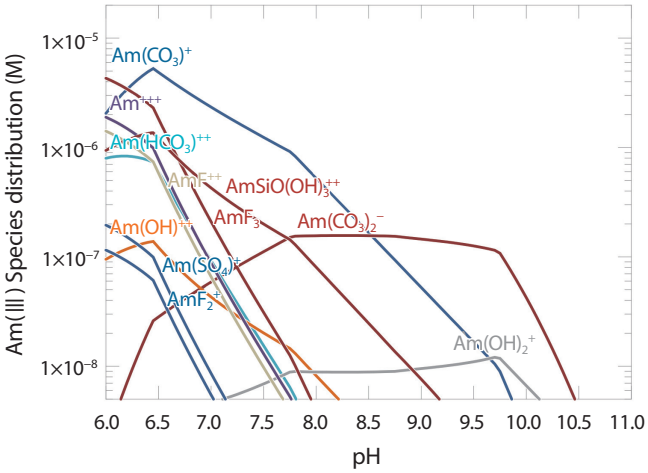


Fig. 2. Geochemical modeling result of aqueous Am(III) species distribution in Syn-DB3 condition. Concentration of americium was set as 11.8 μM. As in Fig. 1(c), formation of crystalline $AmCO_3OH$(cr), $AmCO_3OH:0.5H_2O$(s), and $Am(OH)_3$(cr) was excluded.

excluding crystalline phases with low solubility in the order shown in Figs. 1(a)–1(d).

The modeling results under oxidizing and reducing conditions (Eh −0.5~0.5 V) were the same because americium is stable in the +3 oxidation state under these conditions. Under the Syn-DB3 condition at pH 9, the $AmCO_3OH$ solid compound appeared as the major solubility-limiting phase, with crystallinity-dependent dissolved americium concentrations in the order of $AmCO_3OH$(cr) (~10^{-12} M) < $AmCO_3OH:0.5H_2O$(cr, hyd) (~10^{-9} M) < $AmCO_3OH$(am) (~10^{-7} M) (Fig. 1). In the pH range of 7–10, the main dissolved chemical species were predicted to be $Am(CO_3)^+$ and $Am(CO_3)_2^-$. $AmSiO(OH)_3^{2+}$ was distributed within 10% of the total (Fig. 2). Under weakly acidic conditions, the major chemical species were predicted to be Am^{3+}, AmF_3, and

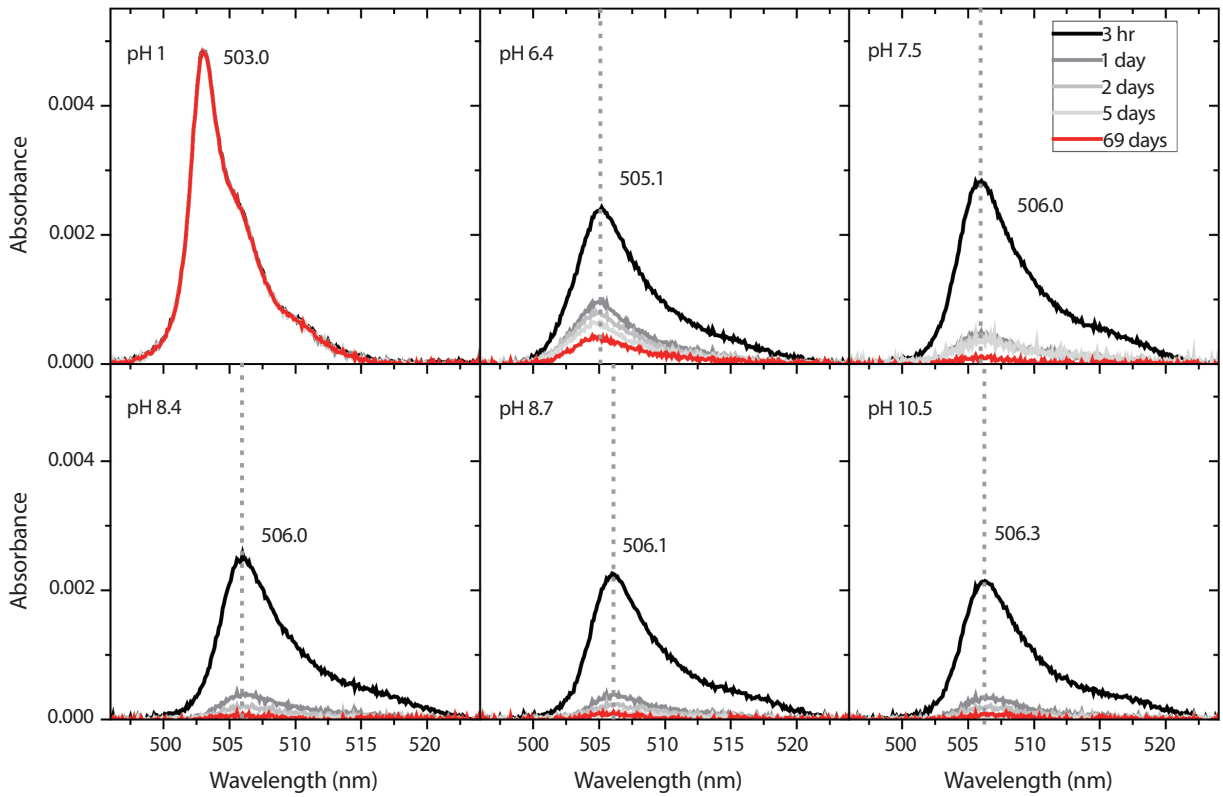


Fig. 3. Aging time-dependent absorption spectra of the Am(III) samples in Syn-DB3 groundwater at various pH of 6.5–10.5. For the reference absorption spectrum, the pH 1 sample in 0.1 M $HClO_4$ was used.

AmF_2^+, whereas $Am(OH)_2^+$ species appeared under alkaline conditions.

3.2 Absorption Spectra of Am (III) in Synthetic Groundwater

The absorption spectrum of Am^{3+} under acidic conditions is well characterized by two major peaks at 503 nm ($\varepsilon = 424 \pm 8$ $cm^{-1} \cdot M^{-1}$) [13-14] and 813 nm ($\varepsilon = 68 \pm 4$ $cm^{-1} \cdot M^{-1}$) [10, 17-18]. The absorption spectra of Am(III) in the Syn-DB3 groundwater were monitored over 69 d (Fig. 3). The first measurement was performed 3 h after sample preparation. The Am(III) sample in 0.1 M $HClO_4$ (pH 1) showed the characteristic absorption spectra of aqua Am^{3+} centered at 503 nm, and there was no change throughout the observation period, confirming that our experimental conditions were stable for the duration. All the Am(III) samples in Syn-DB3 showed gradually red-shifted absorption spectra as pH increased; absorption peaks at 505.1 (pH 6.4), 506.0 (pH 7.5 and 8.4), 506.1 (pH 8.7), and 506.3 nm (pH 10.5). The absorption peak positions of the samples in the pH range of 7.5–8.7 were almost identical, and pH 10.5 also showed a very close peak position despite large differences in the pH values. These results suggest that the absorption peaks at approximately 506 nm originate from Am(III) colloidal particles. This is consistent with our previous findings on Am(III)-OH [13] and -CO_3 systems [19], where Am(III) colloidal particles formed under neutral to alkaline pH conditions showed absorption peaks at approximately 506 nm, but were not luminescent. Similarly, the absorption spectra of Am(III)-humic colloidal systems have also been reported to exhibit absorption peaks at ~506 nm [20-21].

All Am(III)_Syn-DB3 samples showed a rapid decrease in absorbance at 506 nm in 1 d, followed by a continuous decrease over 69 d (Fig. 4), but there was no change in the peak position of each sample (Fig. 3). These observations indicated that Am(III)-colloidal particles were initially formed when the samples were prepared, and the decreased

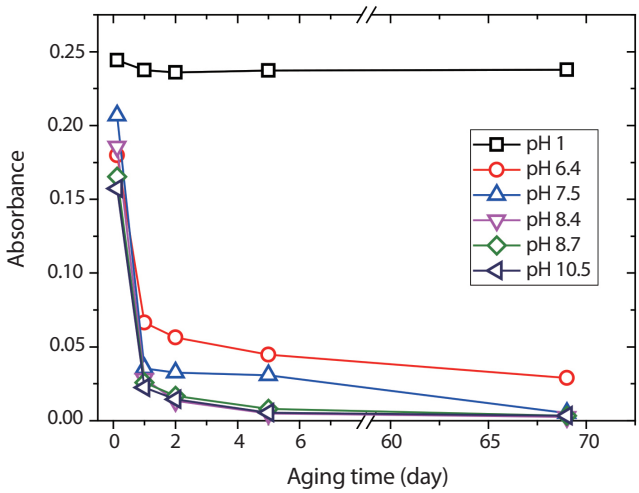


Fig. 4. Aging time-dependent absorption changes (absorption area between 505–515 nm) of the Am(III) in Syn-DB3 groundwater.

absorbance was due to the precipitation of colloidal particles. It is noteworthy that pH 6.4 showed an absorption peak at a different position (505.1 nm) and residual absorbance was still observed after 69 d (Figs. 3 and 4). According to our previous work, ~10 μM Am(III) in 0.1 M $NaClO_4$ at pH ~6.4 showed the same absorption spectrum as in pH 1 solution [13-14]. Thus, the observed absorption at 505.1 nm in the sample at pH 6.4 suggests the formation of aqueous Am(III) complexes with ligands in Syn-DB3, such as $AmCO_3^+$, as predicted by geochemical modeling (Fig. 1).

3.3 Luminescence Properties

The luminescence spectra of Am(III) in Syn-DB3 were acquired 1 d after the preparation. The Am(III) sample at pH 1 showed a luminescence peak at 688 nm, which is well known for aqueous Am^{3+} (Fig. 5) [22-23]. Am(III) in Syn-DB3 samples at pH ≥ 7.5 showed no detectable luminescence signals (Fig. 5), while they still showed detectable absorbance on the same day (1 d), as shown in Figs. 3 and 4. Generally, aqueous Am(III) complexes exhibit red-shifted luminescence with considerably increased intensity [14-15, 24-25], whereas colloidal particles do not exhibit luminescence properties [13-14]. Thus, the absence

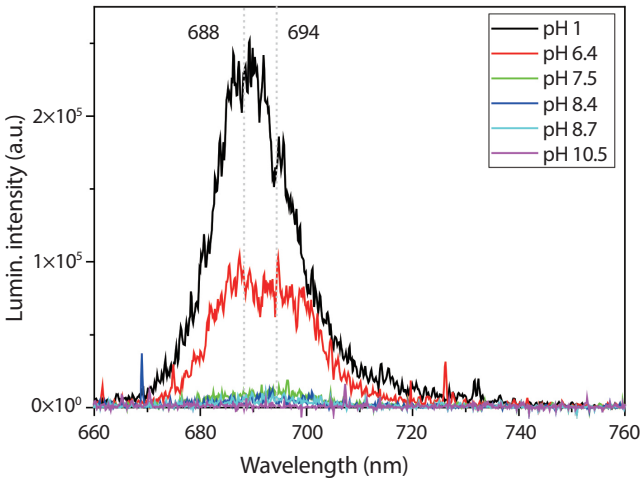


Fig. 5. Luminescence spectra of Am(III) in Syn-DB3 groundwater acquired 1 d after sample preparation.

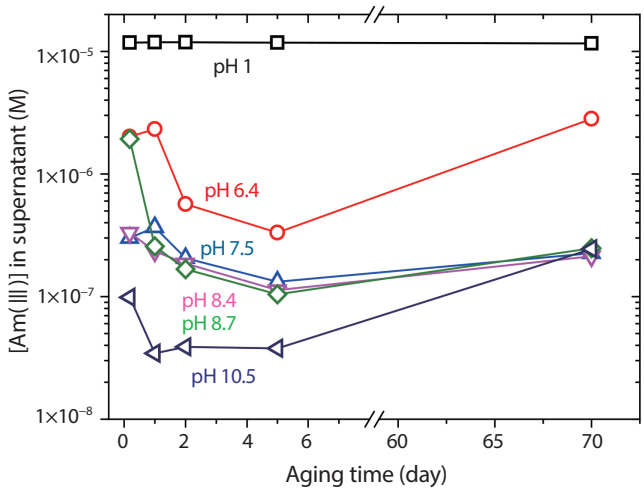


Fig. 6. Sample aging time-dependent americium concentrations in supernatant.

of luminescence from Am(III) in Syn-DB3 samples at pH ≥ 7.5, also indicates that the absorbance at 506 nm is due to the colloidal particles. However, the sample at pH 6.4 showed an additional peak at approximately 694 nm, although the overall luminescence intensity was almost half of that of the pH 1 sample. Luminescence centered at 694 nm has been reported for aqueous Am(III) complexes [14-15]. Thus, the result additionally supports that a small portion of aqueous Am(III) complexes, possibly $AmCO_3^+$, was distributed along with solid phases in the pH 6.4 sample. Further studies are needed to identify these aqueous species.

3.4 Solubility of Americium in Syn-DB3 Groundwater

Am(III) concentrations in the supernatants of the samples were quantified by LSC measurements after centrifugation of the samples at 18,000 rpm for 1 h. Colloidal particles of small sizes might not have completely settled by centrifugation and contributed to concentrations in the supernatant. Therefore, the experimentally measured concentrations of dissolved americium in this study are slightly overestimated. On the day of preparation, the first measurements were conducted in 4.5 h. As shown in Fig. 6, dissolved americium concentrations in Syn-DB3 groundwater at pH range of 6.4–10.5 were measured to be significantly lower than that in americium in 0.1 M $HClO_4$ (1.18×10^{-5} M). Samples at pH 6.4 and 8.7, showed approximately $1/10^{th}$ concentrated americium in the supernatants, and samples at pH 7.5, 8.4, and 10.5, contained only $1/100^{th}$ concentrated americium in the supernatants. Five days after preparation, the americium concentrations in the supernatants decreased to 3×10^{-7} M for the pH 6.4 sample, 1×10^{-7} M for pH 7.5–8.7 samples, and 4×10^{-8} M for the pH 10.5 sample. Interestingly, americium concentration increased back to 3×10^{-6} M for the pH 6.4 sample at 70 d. The concentrations of samples at pH 7.5–10.5 also increased and converged to 2×10^{-7} M in 70 d. The increasing concentrations in the supernatant after 70 d suggest that initially colloidal particles were over-formed owing to the abrupt introduction of americium into the groundwater, and a slow equilibrium process occurred between the aqueous species and the precipitates as sample aging progressed.

In comparisons to modeling results, the measured dissolved americium concentrations at pH 8.4 and 8.7 were significantly higher than those predicted by formation of crystalline $AmCO_3OH$(cr) and $AmCO_3OH{:}5H_2O$(cr, hyd) (Figs. 1(a) and 1(b)). These values were comparable to

those of $AmCO_3OH$(am) (Figs. 1(c) and 1(d)). Unfortunately, we were not able to set up experiments for characterization of the precipitates because the amount of americium in the stock was not sufficient for solid characterization. This is also the reason for performing the over-saturation experiments.

Under over-saturation conditions, fresh precipitates are initially amorphous, which can transform into more crystalline compounds with aging. Thus, it is reasonable that our experimentally determined solubility values follow the solubility of amorphous $AmCO_3OH$(am) rather than that of the crystalline phases ($AmCO_3OH$(cr) and $AmCO_3OH:0.5H_2O$(cr, hyd)). Interestingly, the solubility showed an increasing tendency over time rather than a decreasing trend (5 vs. 70 d), which implies that the amorphous solid state did not transform into a less soluble crystalline form, at least in our observation time window. This suggests that the transformation of the amorphous state to the crystalline state may be required to overcome the high energy barrier, which is too high to be overcome at ambient temperatures. However, temperature-dependent studies are required to test this hypothesis. Our results also underline that kinetic information on solid-state formation and maturation processes is needed for a more reliable prediction of the dissolved concentration and mobility of radionuclides.

The measured dissolved americium concentrations were lower at pH 6.4 and 7.5, than those for the simulation results, while it was higher at pH 10.5 than that for the simulation result. Furthermore, pH 6.4 and 10.5 samples showed increase in the dissolved americium concentrations by almost one order of magnitude in 70 d, by which the pH 6.4 sample approached the solubility line of $Am_2(CO_3)_3$(s) and the pH 10.5 sample to that of $AmCO_3OH$(am) instead of $Am(OH)_3$(am) (Fig. 1 (d)). Overall, samples at pH 7.5–10.5 approached the $AmCO_3OH$(s) solubility in 70 d. As the colloidal americium particles and precipitates matured over time, their physicochemical properties, including particle size and structure, presumably changed, which could accompany the pH changes in the samples and thus cause equilibrium shifts. Indeed, we have often observed time-dependent pH changes in solutions containing americium colloidal particles in an Am(III)-OH system (data not shown). A more systematic and long-term study of americium solubility with close monitoring of solution conditions, including pH and temperature, is needed.

4. Conclusions

The solubility of americium was estimated under over-saturation conditions in Syn-DB3 groundwater. The absorption and luminescence spectroscopic data indicated that colloidal Am(III) particles initially formed and precipitated rapidly over a couple of days. The measured solubility of americium in the Syn-DB3 groundwater condition was comparable to that controlled by amorphous $AmCO_3OH$(am) instead of crystalline phases, when compared with the geochemical modeling results. Our results suggested that kinetic information on the transformation into or between different solid phases was an important factor for predicting the solubility of radionuclides. In addition, our study demonstrated that geochemical modeling results should be interpreted in conjunction with experimental results for a more reliable evaluation of radionuclide mobility. A long-term study of americium solubility with close tracking of the pH changes, tight control of temperatures, and better phase separation, such as ultrafiltration, was needed for a more reliable description of Am behavior in domestic groundwater.

Acknowledgements

This research was supported by the Nuclear Research and Development Program of the National Research Foundation of Korea (Grant Nos. 2021M2E1A1085202 and 2022M2D2A1A02063990).

Disclosure and conflicts of interests

There are no conflicts to declare.

REFERENCES

[1] J.I. Kim, "Significance of Actinide Chemistry for the Long-Term Safety of Waste Disposal", Nucl. Eng. Technol., 38, 459-482 (2006).

[2] R. Guillaumont, T. Fanghänel, V. Neck, J. Fuger, D. Palmer, I. Grenthe, and M.H. Rand, Chemical Thermodynamics Vol. 5: Update on the Chemical Thermodynamics of Uranium, Neptunium, Plutonium, Americium, and Technetium, Elsevier, Amsterdam (2003).

[3] H. Geckeis, J. Lützenkirchen, R. Polly, T. Rabung, and M. Schmidt, "Mineral–Water Interface Reactions of Actinides", Chem. Rev., 113(2), 1016-1062 (2013).

[4] M. Altmaier, X. Gaona, and T. Fanghänel, "Recent Advances in Aqueous Actinide Chemistry and Thermodynamics", Chem. Rev., 113(2), 901-943 (2013).

[5] W. Runde, "The Chemical Interactions of Actinides in the Environment", Los Alamos Science, 26, 392-411 (2000).

[6] I. Grenthe, X. Gona, A.V. Plyasunov, L. Rao, W.H. Runde, B. Grambow, R.J.M. Konings, A.L. Smith, and E.E. Moore. Chemical Thermodynamics Vol. 14: Second Update on the Chemical Thermodynamics of Uranium, Neptunium, Plutonium, Americium, and Technetium, OECD Nuclear Energy Agency Report (2020).

[7] M. Grivé, L. Duro, E. Colàs, and E. Giffaut, "Thermodynamic Data Selection Applied to Radionuclides and Chemotoxic Elements: An Overview of the Thermo-Chimie-TDB", Appl. Geochemistry, 55, 85-94 (2015).

[8] E. Giffaut, M.M. Grivé, P. Blanc, P. Vieillard, E. Colàs, H. Gailhanou, S. Gaboreau, N. Marty, B. Madé, and L. Duro, "Andra Thermodynamic Database for Performance Aassessment: ThermoChimie", Appl. Geochemistry, 49, 225-236 (2014).

[9] H.J. Ervanne, M.E. Hakanen, and E.J. Puukko. Safety Case for the Disposal of Spent Nuclear Fuel at Olkiluoto: Radionuclide Migration Parameters for the Geosphere, Posiva Report, Vol.2012/41 (2014).

[10] J.J. Katz, G.T. Seaborg, and L.R. Morss, The Chemistry of the Actinide Elements, 2nd ed., Springer, New York (1986).

[11] W. Runde, "Americium and Curium: Radionuclides", in : Encyclopedia of Inorganic and Bioinorganic Chemistry, John Wiley & Sons, Ltd., New Jersey (2006).

[12] International Atomic Energy Agency. "Live Chart of Nuclides-Nuclear Structure and Decay Data." IAEA-Nuclear Data Section. Accessed Oct. 15 2022. Available from: https://www-nds.iaea.org/relnsd/vcharthtml/VChartHTML.html.

[13] H.K. Kim, H.R. Cho, E.C. Jung, and W. Cha, "Radioanalytical and Spectroscopic Characterizations of Hydroxo- and Oxalato-Am(III) Complexes", J. Nucl. Fuel Cycle Waste Technol., 16(4), 397-410 (2018).

[14] H.K. Kim, K. Jeong, H.R. Cho, E.C. Jung, K. Kwak, and W. Cha, "Spectroscopic Speciation of Aqueous Am(III)–Oxalate Complexes", Dalton Trans., 48(27), 10023-10032 (2019).

[15] H.K. Kim, K. Jeong, H.R. Cho, K. Kwak, E.C. Jung, and W. Cha, "Study of Aqueous Am(III)-Aliphatic Dicarboxylate Complexes: Coordination Mode-Dependent Optical Property and Stability Changes", Inorg. Chem., 59(19), 13912-13922 (2020).

[16] E.C. Jung, H.R. Cho, M.H. Baik, H. Kim, and W. Cha, "Time-resolved Laser Fluorescence Spectroscopy of $UO_2(CO_3)_3^{4-}$", Dalton Trans., 44(43), 18831-18838 (2015).

[17] S.E. Stephanou, J.P. Nigon, and R.A. Penneman, "The Solution Absorption Spectra of Americium(III), (V), and (VI)", J. Chem. Phys., 21, 42-45 (1953).

[18] T.K. Keenan, "Americium and Curium", J. Chem. Educ., 36(1), 27-31 (1959).

[19] H.K. Kim, "Spectroscopic Characterizations of Aqueous and Colloidal Am(III)-CO_3 Complexes for

Monitoring Species Evolutions", J. Nucl. Fuel Cycle Waste Technol., 20(4), in press (2022).

[20] J.I. Kim, D.S. Rhee, and G. Buckau, "Complexation of Am(III) With Humic Acids of Different Origin", Radiochim. Acta, 52-53(1), 49-55 (1991).

[21] M. Morgenstern, R. Klenze, and J.I. Kim, "The Formation of Mixed-Hydroxo Complexes of Cm(III) and Am(III) With Humic Acid in the Neutral pH Range", Radiochim. Acta, 88(1), 7-16 (2000).

[22] J.V. Beitz, G. Jursich, and J.C. Sullivan, "Fluorescence Studies of Am^{3+} in Aqueous Solution", J. Less- Common Met., 126, 301 (1986).

[23] J.V. Beitz, "f-State Luminescence of Trivalent Lanthanide and Actinide Ions in Solution", J. Alloys Compd., 207-208, 41-50 (1994).

[24] A. Barkleit, G. Geipel, M. Acker, S. Taut, and G. Bernhard, "First Fluorescence Spectroscopic Investigation of Am(III) Complexation With an Organic Carboxylic Ligand, Pyromellitic Acid", Spectrochim. Acta A Mol. Biomol. Spectrosc., 78(1), 549-552 (2011).

[25] B. Raditzky, S. Sachs, K. Schmeide, A. Barkleit, G. Geipel, and G. Bernhard, "Spectroscopic Study of Americium(III) Complexes With Nitrogen Containing Organic Model Ligands", Polyhedron, 65, 244-251 (2013).